Soluble levels of cytosolic tubulin regulate ciliary length control

Neeraj Sharma, Zachary A. Kosan, Jannese E. Stallworth, Nicolas F. Berbari, and Bradley K. Yoder
Department of Cell Biology, School of Medicine, University of Alabama at Birmingham, Birmingham, AL 35294

ABSTRACT **The primary cilium is an evolutionarily conserved dynamic organelle important for regulating numerous signaling pathways, and, as such, mutations disrupting ciliogenesis result in a variety of developmental abnormalities and postnatal disorders. The length of the cilium is regulated by the cell through largely unknown mechanisms. Normal cilia length is important, as either shortened or elongated cilia have been associated with disease and developmental defects. Here we explore the importance of cytoskeletal dynamics in regulating cilia length. Using pharmacological approaches in different cell types, we demonstrate that actin depolymerization or stabilization and protein kinase A activation result in a rapid elongation of the primary cilium. The effects of pharmacological agents on cilia length are associated with a subsequent increase in soluble tubulin levels and can be impaired by depletion of soluble tubulin with taxol. In addition, subtle nocodazole treatment was able to induce ciliogenesis under conditions in which cilia are not normally formed and also increases cilia length on cells that have already established cilia. Together these data indicate that cilia length can be regulated through changes in either the actin or microtubule network and implicate a possible role for soluble tubulin levels in cilia length control.**

Monitoring Editor
Monica Bettencourt-Dias
Instituto Gulbenkian de Ciência

Received: Mar 31, 2010
Revised: Jan 5, 2011
Accepted: Jan 13, 2011

INTRODUCTION

Microtubules (MTs) and actin are dynamic components of the structural network within a cell, and they regulate important processes, including cell shape, migration, cytokinesis, and vesicular transport (Rodriguez *et al.*, 2003). Together, MT and actin networks are important for cellular responses and signal transduction through their influence on channel and receptor transport, function, and localization (Johnson and Rosenbaum, 1993; Saunders and Limbird, 1997; Goswami *et al.*, 2004; Montalbetti *et al.*, 2005; Li *et al.*, 2006; Montalbetti *et al.*, 2007). The dynamic nature of MTs results in pools of polymerized and unpolymerized tubulin in the cytosol (Mitchison and Kirschner, 1984). In addition to the dynamic population of MTs, there is a fraction of stable MTs, often marked by posttranslational modifications, such as tubulin acetylation, glycylation, and glutamylation, that turn over relatively slowly (Gundersen *et al.*, 1984; Webster *et al.*, 1987). These modifications can also influence kinesin motors and alter transport processes (Ikegami *et al.*, 2007; Konishi and Setou, 2009; Hammond *et al.*, 2010).

MT assembly is coordinated by the centrosome that functions as the MT-organizing center (MTOC). The centrosome also forms the basal body that serves as a template for extension of the microtubules during ciliogenesis, thus connecting the axoneme of the cilium with the MT cytoskeleton. In dividing cells, the cilium and its MT axoneme must be retracted to release the centrosome/centrioles to form the mitotic spindle (Tucker *et al.*, 1979; Quarmby and Parker, 2005; Pugacheva *et al.*, 2007), and subsequently the cilium and cytoskeletal MT must be reassembled during cell quiescence.

Cilium extension from the basal body and subsequent maintenance requires intraflagellar transport (IFT). IFT involves molecular motors that attach to a large complex of proteins (IFT particle) mediating the bidirectional movement of cargo along the polarized microtubules of the axoneme (Kozminski *et al.*, 1993; Scholey, 2003). Defects in the cilia assembly process, its signaling components, or ciliary length have been associated with severe developmental abnormalities and diseases, collectively known as ciliopathies (Fliegauf *et al.*, 2007; Sharma *et al.*, 2008). For example, renal cystic disease has been associated with excessively long cilia, as seen in *bbs-4* (Mokrzan *et al.*, 2007), *mks-3* (Tammachote *et al.*, 2009), and *nek-8* (Sohara *et al.*, 2008) mutants; shortened or elongated cilia in hypomorphic *ift88*^{orpk} mutant and rescued mice (Murcia *et al.*, 2000); and

This article was published online ahead of print in MBoC in Press (http://www.molbiolcell.org/cgi/doi/10.1091/mbc.E10-03-0269) on January 26, 2011.

Address correspondence to: Bradley K. Yoder (byoder@uab.edu).

Abbreviations used: CD, cytochalasin D; IFT, intraflagellar transport; Jasp1, Jasplakinolide; MT, microtubule; PTM, posttranslational modifications.

complete cilia loss, as seen in the kidney-specific conditional IFT mutants (Jonassen *et al.*, 2008; Sharma and Yoder, unpublished data). Although the significance of this organelle for normal tissue function and development is now well appreciated, how the length of the cilium affects tissue physiology and the molecular mechanisms controlling ciliary length remains poorly defined.

Cilia/flagella length control has been best studied in model organisms such as *Chlamydomonas*, in which the size of each flagellum is under genetic control and several genes involved in the regulation of flagella length have been identified (Asleson and Lefebvre, 1998; Tuxhorn *et al.*, 1998; Wilson and Lefebvre, 2004; Wemmer and Marshall, 2007). In *Chlamydomonas*, flagella length may be related to IFT as there is an inverse relationship between cilia/flagella length and the size and possibly frequency of IFT particles entering and leaving the cilium (Iomini *et al.*, 2001; Engel *et al.*, 2009). In mammalian cells, a recent study revealed that a decrease in calcium or an increase in cyclic AMP (cAMP) can cause cilia elongation (Besschetnova *et al.*, 2010). These processes may be related as numerous phosphodiesterases (PDE) are calcium-inhibited and could subsequently also alter cAMP levels. Although the exact mechanism is unknown, cAMP mediates this effect on cilia length through the activation of protein kinase A (PKA), and in mammalian cells this has been associated with increased anterograde rates of IFT (Besschetnova *et al.*, 2010). Thus, similar to what was reported in *Chlamydomonas*, the regulation of cilia length in mammals may involve altering the rates of delivery, retention, or retraction of ciliary components mediated through IFT. With regard to cAMP, it is intriguing that cystic kidney diseases in humans and rodent models are associated with elevated levels of cAMP (Yamaguchi *et al.*, 1997; Torres *et al.*, 2004; Smith *et al.*, 2006). This could provide an explanation as to why there is a marked increase in cilia length observed in some of the cystic models that do not directly involve mutations in IFT genes (Smith *et al.*, 2006; Mokrzan *et al.*, 2007; Tammachote *et al.*, 2009).

In addition to cAMP and its potential effects on IFT, several recent studies in mammalian cells have indicated that changes in cytoskeletal dynamics also affect cilia length. A study by Kim *et al.*, using a small-molecule approach has identified several factors that alter the activity of proteins known to regulate actin organization (Kim *et al.*, 2010). These include two gelsolin family members (GSN and AVIL) that are important in actin filament severing and ARP3/ACTR3, which promotes actin polymerization at filament branches. Knockdown of GSN and AVIL caused an inhibition of ciliogenesis, whereas disruption of ARP3/ACTR3 resulted in elongated cilia. The importance of the actin cytoskeleton was further demonstrated by treating cells with the actin polymerization inhibitor cytochalasin D (CD), which also caused elongation of cilia. Intriguingly, this was associated with enhanced formation of a vesicular structure called the preciliary compartment (PCC) at the basal body. These data suggested that the PCC was a site of vesicle docking at the base of the cilium, where it functioned as a temporary reservoir of lipid and ciliary membrane proteins. They proposed a mechanism whereby the actin cytoskeleton inhibits cilia growth through destabilization of the PPC and the effect of actin destabilization on cilia length was a result of increased membrane transport into the cilium.

Alterations in tubulin cytoskeletal dynamics have also been associated with changes in cilia or flagella size. For example, disruption of katanin, a microtubule-severing protein, in *Tetrahymena* was shown to cause stunted cilia and impaired ciliogenesis (Sharma *et al.*, 2007). In addition, the rate of flagella growth in *Chlamydomonas* correlates directly with the activity of the microtubule depolymerizing kinesin CrKinesin-13, and disruption of its activity leads to defects in ciliogenesis and flagella regeneration (Piao *et al.*, 2009).

A connection between the cilium and the cytoskeleton is also supported by ciliary proteins that have been implicated in cystic kidney disorders, such as PKD-2, and Meckel-Gruber syndrome (MKS). PKD-2, which is disrupted in nearly 15% of human polycystic kidney disease (PKD) patients, was recently found to interact with several cytoskeletal components (Rundle *et al.*, 2004; Montalbetti *et al.*, 2005; Chen *et al.*, 2008). The ciliary proteins MKS1 and Meckelin (MKS3) are known to interact with nesprin-2, a scaffold protein involved in maintenance of the actin cytoskeleton (Dawe *et al.*, 2009). In addition, depletion of Meckelin by small, interfering RNA (siRNA) leads to actin reorganization and defects in centriole/basal body migration and/or docking at the cell membrane prior to ciliogenesis.

The basic subunits of cilia axoneme are α- and β-tubulin. These subunits are synthesized in the cell body (Szymanski, 2002; Gaertig and Wloga, 2008), and anterograde IFT transports these components to the distal ends of the outer doublets, where they are then incorporated into the cilia axoneme. Retrograde IFT is also important for transport of recycled components back to the cytosol (Pazour *et al.*, 1998; Blacque *et al.*, 2006; Absalon *et al.*, 2008). Thus in addition to modulating cilia length through IFT regulation, the cell may be able to influence the length of the cilium by controlling the levels of soluble tubulin needed to build the cilia axoneme. Indeed, studies in *Chlamydomonas* have shown that tubulin levels are markedly up-regulated in response to deflagellation (Weeks and Collis, 1976; Silflow and Rosenbaum, 1981) and that altered microtubule dynamics in the cell body may have a crucial role in flagella regeneration (Piao *et al.*, 2009). However, this has not been evaluated carefully in the context of mammalian cells nor has there been an association made between cytoskeleton and cAMP-induced cilia elongation.

Here we used a pharmacological approach with distinct mouse and human cell types to demonstrate that cilia length can be influenced by changes in the dynamics of the actin and microtubule cytoskeleton and that these changes are associated with increased levels of soluble tubulin. These findings provide a connection between the polymeric state of cell body microtubules and the regulation of cilia length, and establish the basis for future investigations into how fundamental changes in cytoskeletal elements, such as actin and tubulin, may be involved in some of the clinical features observed in ciliopathies.

RESULTS

Changes in actin cytoskeleton affect primary cilia length

Several recent studies have uncovered a connection between disruption of the actin cytoskeleton and cilia length control (Bershteyn *et al.*, 2010; Kim *et al.*, 2010); however, the downstream effects that contribute to cilia elongation remained uncertain. Here we explore this issue using multiple cell types and provide data indicating that the ciliary length increase in response to actin depolymerization is associated with increased levels of soluble tubulin.

To confirm previous data by Kim *et al.* and test the conservation of the effect, we disrupted the actin cytoskeleton with CD in human retinal pigmented epithelium (htRPE) cells, mouse inner medullary collecting duct (IMCD) cells, renal epithelium (CAGGCre; Kif3a$^{fl/fl}$) cells (see *Materials and Methods* for details), mouse embryonic fibroblasts (MEFs), and in an ex vivo whole mouse kidney culture. Ciliogenesis in IMCD and Kif3a$^{fl/fl}$ cells is not dependent on serum-starvation conditions; however, htRPE cells and MEFs will uniformly form cilia only following serum deprivation. Cells were treated with

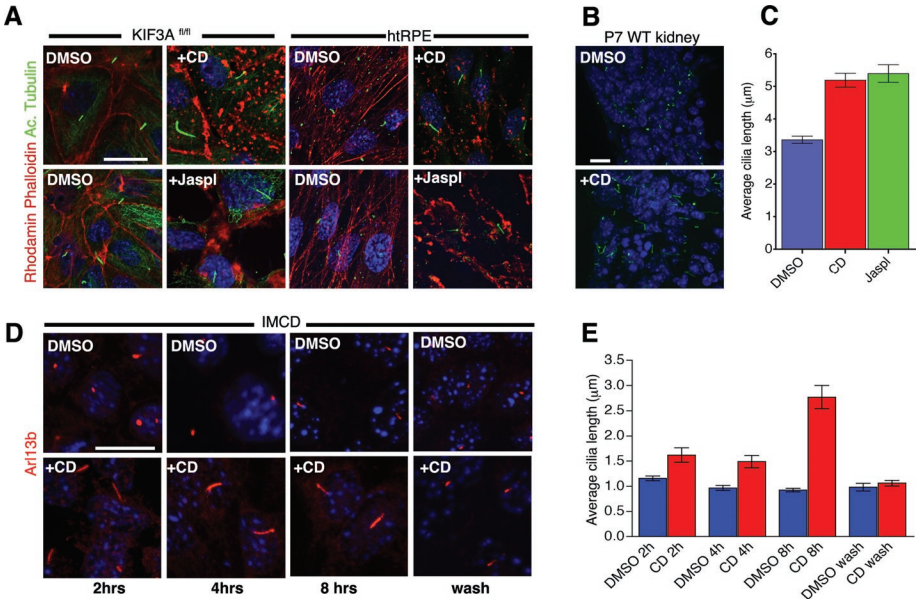

FIGURE 1: Depolymerization and stabilization of the actin cytoskeleton causes cilia elongation. (A) Kif3a$^{fl/fl}$ renal collecting duct and htRPE cells treated with 1 μM CD or 1 μm Jasplakinolide (Jaspl) resulted in cilia elongation. Actin cytoskeleton was stained with rhodamine phalloidin (red), and cilia were stained with acetylated tubulin (green). (B) Cryosections of WT kidneys from 7-d-old mice that were treated ex vivo with 1 μm CD resulted in elongated cilia as detected by staining with anti-Arl13b (green). (C) Quantification of htRPE cilia length increase when treated with 1 μM CD or 1 μM Jaspl. Mean cilia length for DMSO (3.38 ± 0.113 μm), CD (5.19 ± 0.213 μm), and Jaspl (5.4 ± 0.27 μm). Values as mean ± SEM. (D) IMCD cells were treated with 1 μM CD for 2, 4, and 8 h and stained for cilia by anti-Arl13b (red) antibody. Cilia elongation was apparent within 2 h of CD treatment and returned to normal length within an hour after CD removal (lower right subpanel). (E) Quantification of IMCD cilia length increase over time in the presence of CD. All scale bars 15 μm and nuclei stained in blue by Hoechst.

1 μM CD for 2–4 h and stained with rhodamine-phalloidin and anti-acetylated tubulin. Actin depolymerization in Kif3a$^{fl/fl}$ cells (serum present), IMCD (serum present), and htRPE cells (without serum) resulted in significant elongation of the primary cilium compared with dimethyl sulfoxide (DMSO) treatment (Figure 1, A, C, and D). Similarly, treating renal explants with CD also led to a marked elongation of cilia (Figure 1B). Collectively, these data show that perturbation of the actin cytoskeleton results in a rapid increase in cilia length across multiple cell types.

In cultured cells, we also detected a higher frequency of multinucleated cells with multiple cilia per cell after treating with CD for 24 h (Supplemental Figure S1). In these cases, both of the cilia were elongated relative to the untreated controls. Formation of multiciliated cells could be blocked by serum starvation to inhibit cell proliferation prior to CD treatment (data not shown). These data indicate that multiciliated cells are likely a consequence of defects in cell division associated with actin depolymerization, whereas the effects on cilia length control are independent of cell division.

We next analyzed the temporal effects of the actin cytoskeleton on cilia by assessing how rapidly cilia elongation occurs after CD treatment and the rate at which cilia length returns to baseline after CD is removed. Interestingly, elongated cilia were clearly evident within 2 h of CD treatment and returned to basal length within 1 h of drug removal (Figure 1, D and E). Although CD has multiple effects on the cell, these data support a coupling between the actin cytoskeleton and cilium elongation and are also consistent with data from the genomic screen (Kim *et al.*, 2010).

Previous work has shown that actin localizes to cilia in nonmammalian cells (Chaitin *et al.*, 1984; Chailley *et al.*, 1986; Muto *et al.*, 1994; Watanabe *et al.*, 2004). However, we could not detect actin in primary cilia of our cell lines when stained with rhodamine-phalloidin (Figure 1A) or using a polyclonal anti-actin antibody (Supplemental Figure S2). These data suggest that actin depolymerization/stabilization-mediated effects on cilia length are indirect and that this occurs in the cell body itself.

Because actin depolymerization causes cilia elongation, we asked whether actin stabilization might promote cilia shortening or complete disassembly. Jaspl stabilizes actin filament by binding to three-monomer subunits along the length of the filament (Bubb *et al.*, 1994, 2000), causes aggregation of actin filaments (Lee *et al.*, 1998), and induces formation of new filaments (Holzinger and Meindl, 1997). We treated Kif3a$^{fl/fl}$, htRPE, and IMCD cells with 1 μM Jaspl for 2 h. Unexpectedly, Jaspl treatment also resulted in cilia elongation similar to what we observed with actin depolymerization (Figure 1, A and C, and Figure 2).

Stabilization of cytoplasmic microtubules inhibits cilia elongation mediated by either disruption or stabilization of the actin cytoskeleton

In previous studies, it has been shown that increasing MT stability through inactivation of katanin, a MT-severing protein, impaired ciliogenesis (Sharma *et al.*, 2007). Thus we next analyzed whether actin depolymerization or actin stabilization may affect cytoplasmic MT dynamics, shifting the equilibrium toward depolymerization and generating "extra soluble tubulin" available for axonemal incorporation. To test this hypothesis, cells were grown to confluence and then serum starved for 72 h to ensure analysis of preexisting cilia. BrdU staining confirmed inhibition of cell proliferation, and most cells were found to possess a primary cilium that was consistently 1–2 μm long (data not shown). Cells were then treated with 1 μm taxol for 2 h to stabilize MT prior to adding CD or Jaspl. As indicated previously, CD or Jaspl treatment alone caused a significant increase in cilia length but did not cause an increase in the percentage of ciliated cells in IMCD and WT Kif3a$^{fl/fl}$ collecting duct cells. Intriguingly, the increase in cilia length induced by CD or Jaspl could be inhibited by pretreatment of cells with taxol (Figure 2 and Figure 3, A and B; see Supplemental Table 1 for CD treatment). Treating serum-starved cells with taxol alone did result in an increase in the frequency of cells lacking cilia (Figures 3B and 4B), and those that were ciliated were somewhat stunted when compared with the cilia in DMSO-treated control cells (Figures 3B and 4B; Supplemental Tables 1 and 2). Thus the elongation of the cilium observed after stabilization or destabilization of the actin network could be inhibited by prior treatment with taxol.

Regulation of cilia length is associated with changes in soluble and insoluble tubulin pools

Taxol binding to tubulin stabilizes MTs, decreasing the pool of free tubulin in the cytosol, thereby reducing the amount of unpolymerized tubulin in cytosol readily available for cilia elongation and

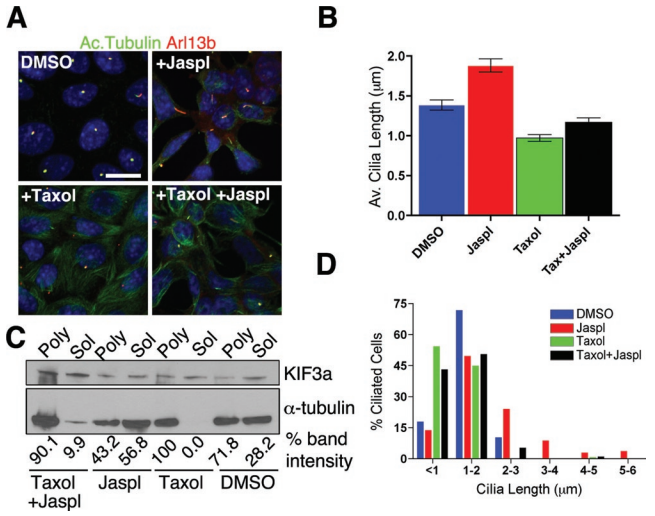

FIGURE 2: Actin-stabilization induced cilia elongation is suppressed by microtubule stabilization. (A) Immunofluorescence analysis of IMCD cells treated with DMSO, taxol (1 μM), Jaspl (1 μM), and taxol (1 μM) + Jaspl (1 μM). Cells were stained with anti-Arl13b (red) and anti-acetylated tubulin (green) to visualize cilia. Then, 1 μM taxol was added 2 h prior to Jaspl treatment. Scale bar 15 μm and nuclei stained in blue by Hoechst. (B) Mean cilia length in various treatments (right bar graph). Mean cilia length for DMSO (1.38 ± 0.06 μm), Jaspl (1.98 ± 0.08 μm), taxol (0.95 ± 0.04 μm), taxol + Jaspl (1.16 ± 0.05 μm). Values as mean ± SEM. (C) Immunoblot analysis of soluble and polymerized tubulin fractions extracted from DMSO, taxol only, Jaspl only, and taxol + Jaspl treatments. Blot was reprobed using anti-Kif3a antibody as loading control. Relative amount of tubulin present in soluble and polymerized fractions in each treatment is represented by percent band intensity. (D) Quantification of percentage of cells with a cilium under different treatments.

maintenance. Furthermore, the ability of taxol to inhibit CD- or Jaspl-meditated cilia elongation suggests a correlation between actin depolymerization and the levels of soluble tubulin pools in the regulation of cilia length. We further analyzed this possible correlation by determining soluble and polymerized tubulin fractions under each of the treatment conditions. In support of the hypothesis, CD-treated cells have a higher amount of soluble tubulin and lower polymerized MTs compared with untreated cells (Figure 3C). In contrast, cells pretreated with taxol and then with CD show low levels of soluble tubulin and a higher fraction of polymerized MTs. Thus CD's effect on cilia length correlates directly with increased levels of free tubulin (Figure 3, B and C), although it must be noted that both CD and taxol have broad affects on the cell that could contribute to cilia regulation and were not evaluated here. The efficacy of the treatment regiment and extraction procedure was assessed using cells treated with nocodazole or taxol. Taxol resulted in a large reduction in the levels of soluble tubulin and a concomitant increase in polymerized tubulin pools. In contrast, nocodazole showed a modest increase in soluble tubulin relative to DMSO under the conditions used in these assays.

Because taxol inhibited Jaspl-induced cilia elongation, we further analyzed the effects of actin stabilization on soluble tubulin levels in the cell body. Interestingly, as observed with actin depolymerization, higher levels of soluble tubulin were detected when actin was stabilized by Jaspl (Figure 2C). Additionally, cells treated with taxol followed by Jaspl showed a higher fraction of polymerized MTs and lower levels of unpolymerized tubulin (Figure 2C). These observations suggest that perturbation of actin dynamics affect microtubule polymers in the cell body, which influence the regulation of cilia length.

Although the mechanisms regulating cilia length control in mammalian cells are still poorly defined, recent data have revealed that cAMP-induced activation of PKA leads to cilia elongation that is associated with increased rate of anterograde IFT (Besschetnova *et al.*, 2010). However, possible effects of PKA activation on the cytoskeleton were not evaluated. Thus we first confirmed the effect of cAMP on cilia length by treating IMCD and Kif3a$^{fl/fl}$ (data not shown) collecting duct cells with 0.05 mM forskolin. As reported, forskolin treatment caused a significant increase in cilia length (Figure 4, A and B); however, there was no apparent disruption of actin cytoskeleton as revealed by rhodamine-phalloidine staining (Supplemental Figure S2). We next evaluated whether blocking microtubule depolymerization was able to impair forskolin-mediated cilia elongation by pretreating cells with 1 μM taxol prior to addition of forskolin. Similar to the results obtained with taxol and CD, the cilia elongation induced by forskolin was attenuated by addition of taxol (Figure 4, A and B, and Supplemental Table 3). However, taxol was not able to completely abolish the forskolin effect, as there was a statistical significant increase in cilia length in the taxol + forskolin–treated cells relative to taxol-alone–treated cells. As observed earlier, in taxol-only–treated samples, >30% of cells failed to assemble cilia (Figure 4B and Supplemental Table 4).

Because forskolin induced cilia elongation that could be impaired by taxol, we evaluated whether these effects on cilia length correlated with levels of soluble and polymerized tubulin. Forskolin treatment caused an increase in cytosolic unpolymerized tubulin (Figure 4C). In contrast, the truncated cilia in taxol-treated cells were associated with a marked reduction in the levels of soluble tubulin (Figure 4C). It should be noted that the levels of soluble tubulin remained somewhat elevated in the taxol + forskolin group compared with taxol alone, but was less than detected with forskolin alone. These effects on soluble tubulin under the different conditions may help explain why cilia length was intermediate in the taxol + forskolin–treated samples. In addition, previous studies by Besschetnova *et al.* (2010) have demonstrated that cAMP also increases the rate of anterograde IFT, which may not be affected by taxol, contributing to the intermediate phenotype.

Our data show that taxol-mediated depletion of unpolymerized tubulin in the cytosol is associated with cilia shortening or complete loss of ciliogenesis. However, it is possible that taxol-induced posttranslational modification (PTM) on MTs could affect the binding of molecular motors involved in intracellular transport (Reed *et al.*, 2006; Hammond *et al.*, 2010). To begin assessing this possibility, we evaluated the effects of Lys40 α-tubulin acetylation on cilia. MEFs were treated with 1 μm tubacin for 4 h (generous gift from Stuart Schreiber, Harvard University) (Haggarty *et al.*, 2003). Control cells were treated with niltubacin, which is an inactive derivative of tubacin (Haggarty *et al.*, 2003). Tubacin is a highly selective inhibitor of HDAC6, an enzyme that is responsible for deacetylation of α-tubulin both in vitro and in vivo (Hubbert *et al.*, 2002). Although tubacin-treated cells showed significant increase in acetylation of cytoplasmic microtubules, it did not affect cilia assembly compared with niltubacin-treated cells (Supplemental Figure S5). Tubacin treatment did not affect polyglutamylation on microtubules (Supplemental Figure S5). These results suggest that an increase in microtubule acetylation in the cell body does not affect cilia length. On the basis of these data, we propose that the effect of taxol on cilia length is related to polymerization state of the microtubules rather than accumulation of PTMs, in this case α-tubulin acetylation.

To further assess the connection between cilia length, PKA, and the cytoskeleton, we analyzed whether PKA inhibition is able to block actin depolymerization-induced cilia elongation. Cells were

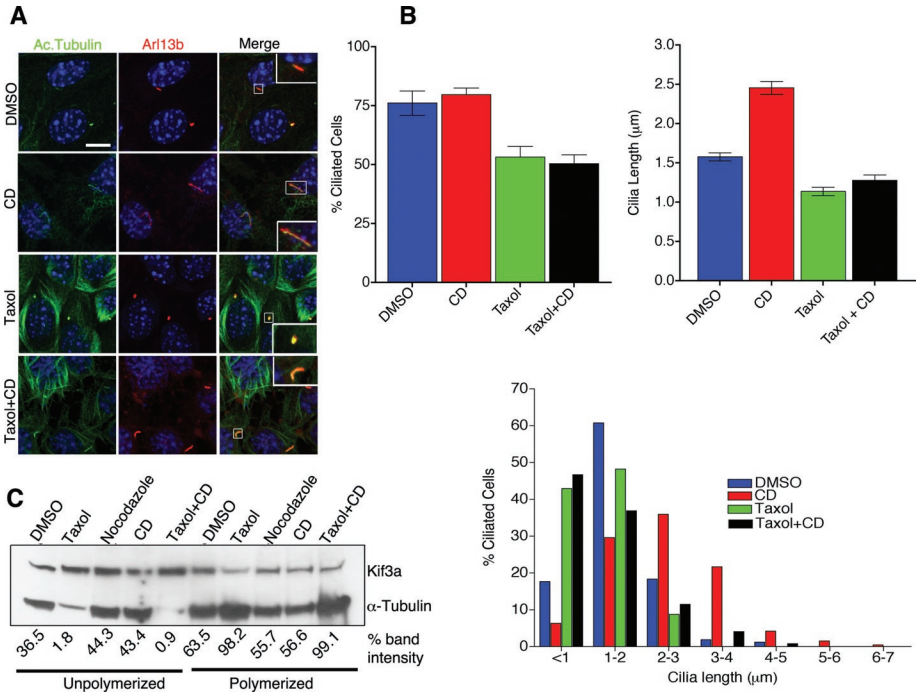

FIGURE 3: Suppression of microtubule depolymerization by taxol inhibits actin depolymerization mediated elongation of cilia. (A) Immunofluorescence analysis of cilia from DMSO, taxol only, CD only, and taxol + CD treated WT Kif3a$^{fl/fl}$ collecting duct cells. Cilia identity was confirmed by double staining with anti-Arl13b (red) and anti-acetylated tubulin (green), and only double-positive structures were considered for cilia length quantification. Scale bar 10 μm and nuclei stained in blue by Hoechst. (B) Measurements of mean cilia length in response to different treatments (right graph). Mean cilia length for DMSO (1.57 ± 0.051 μm), CD (2.5 ± 0.082 μm), taxol (1.14 ± 0.53 μm), and taxol + CD (1.27 ± 0.071 μm). Values as mean ± SEM. Error bars are 95% confidence intervals (see supplemental materials for P values; Table 1). Quantification of percentage of cells with a cilium under different treatments (left graph, supplemental materials for P values; Table 2). Histogram of cilia length distribution in response to different drug treatments (below). (C) Immunoblot analysis of soluble and polymerized tubulin fractions extracted from DMSO, taxol only, CD only, and taxol + CD treatments. Nocodazole treatment was used as a positive control for fractionation. Blot was simultaneously probed for Kif3a and IFT88 (not shown) as loading controls. Relative amount of tubulin present in soluble and polymerized fractions in each treatment is represented by percent band intensity.

preincubated with KT5720, a PKA inhibitor. CD or forskolin was then added to cause actin depolymerization or activation of PKA, respectively. Although treating cells with KT5720 was sufficient to block the forskolin-induced cilia length increase (Figure 5, A and B), it did not block cilia elongation caused by disruption of the actin cytoskeleton (Figure 5, C and D, and Supplemental Table 5). However, we did note an increase in the percentage of cells lacking cilia after treating with KT5720 alone (Figure 5D and Supplemental Table 7) and that it did not by itself alter the average length of the cilium (Figure 5, B and D, and Supplemental Table 6). Furthermore, inhibition of PKA with KT5720 did not result in an increase in acetylated tubulin positive cytosolic MTs (Figure 5, A and C) as we observed in taxol-treated cells (Figures 2A, 3A, and 4A). Together these data suggest that PKA- and actin/tubulin cytoskeleton–mediated effects on cilia length occur through independent pathways, both of which are also associated with increased levels of soluble tubulin.

Nocodazole-mediated depolymerization of cytoplasmic microtubules affects cilia length and induces ciliogenesis under nonciliogenic conditions

Collectively, our data suggest that cytosolic microtubules can influence ciliary length. To evaluate this further, we treated htRPE cells with very low to high amounts of the MT depolymerizing agent nocodazole. Cultured cells treated with micromolar concentrations of nocodazole rapidly depolymerize microtubules and are blocked in mitosis (De Brabander *et al.*, 1976; Lee *et al.*, 1980). However, at nanomolar concentrations of nocodazole, microtubules exhibit slower elongation and decreased velocities accompanied with increased microtubule catastrophe (Vasquez *et al.*, 1997). The mechanism of nocodazole in regulating microtubule dynamics is not clear; however, according to current models, nocodazole affects microtubule dynamics by promoting formation of nocodazole-tubulin dimer and inducing tubulin GTPase activity (Vasquez *et al.*, 1997). Serum-starved htRPE cells (Supplemental Figure S3) and nonstarved WT Kif3a$^{fl/fl}$ (data not shown) were treated with different concentrations of nocodazole for 2 h at 37°C. Intriguingly, treating htRPE cells with 100 nM nocodazole resulted in elongated cilia (3.9 ± 0.14 μm) compared with DMSO-treated cells (1.9 ± 0.15 μm) (Figure 6, A and B, and Supplemental Figure S3). This phenotype was not observed in htRPE cells treated with 10 nM nocodazole, and cilia were not present on htRPE cells treated with 1 μM nocodazole. The effects at higher concentrations of nocodazole are likely due to complete depolymerization of microtubules within the cell body, which would disrupt both the IFT process and cytosolic MT transport in the cell. We further tested whether there is a correlation between amount of soluble tubulin in the cell body and cilia length. To assess this possibility, we treated serum-starved htRPE cells with different doses of nocodazole and fractionated soluble and polymerized tubulin. Treatement with 100 nM nocodazole results in a significant increase in soluble tubulin compared with DMSO-treated cells (Supplemental Figure S3, bar graph). Interestingly, 1 nM and 10 nM nocodazole also affected microtubules, but the levels of depolymerized tubulin were slightly lower than the depolymerized tubulin in 100 nM treatment (blue bar represents soluble tubulin in Supplemental Figure S3; DMSO = 47.1%, 1 nM = 49.2%, 10 nM = 52.6%, 100 nM = 61%, 1 μM = 79.2%). However, 1 μM nocodazole resulted in dramatic reduction in polymerized microtubules that affected ciliogenesis.

htRPE cells normally do not form cilia in the presence of serum. Thus we asked whether subtle microtubule depolymerization could induce cilia formation in htRPE cells cultured with serum. For these studies, htRPE cells were cultured in high-serum medium in the presence of 100 nM nocodazole. These conditions were found to significantly increase the number of ciliated cells (Figure 6, C and D). These observations indicated that ciliogenesis and cilia length regulation may be susceptible to the amount of free tubulin as well as polymerized tubulin in the cell body; however, at this point it is not clear whether this correlation is direct or indirect.

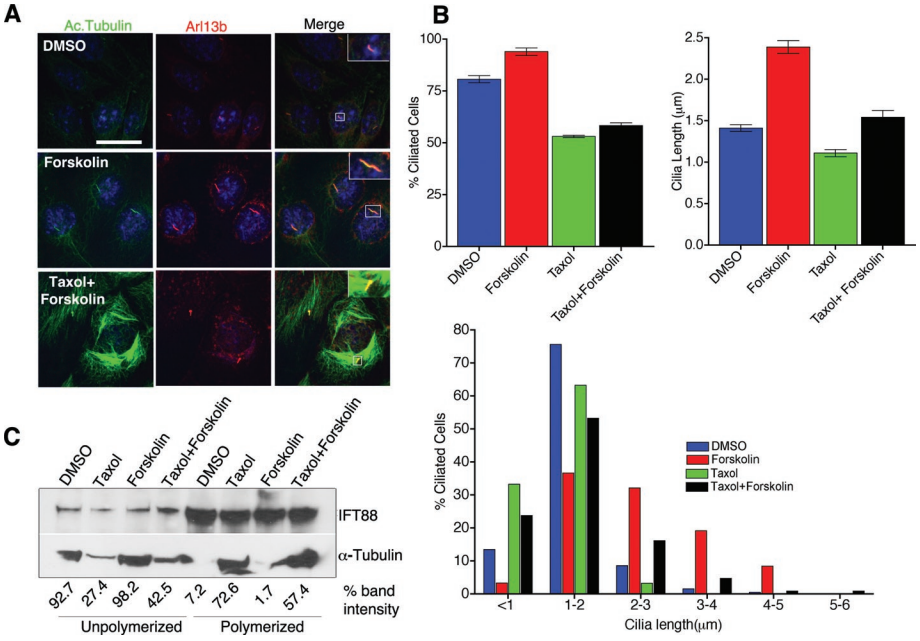

FIGURE 4: Forskolin-induced cilia elongation is inhibited by microtubule stabilization. (A) Immunofluorescence analysis of IMCD cells treated with DMSO, forskolin (0.05 mM), taxol (1 μM), and taxol (1 μM) + forskolin (0.05 mM). Cells were fixed and stained for anti-Arl13b (red), anti-acetylated tubulin (green) to visualize cilia. Then, 1 μM taxol was added 2 h prior to forskolin (−/+) treatment. Scale bar 15 μm and nuclei stained in blue by Hoechst. (B) Mean cilia length in different treatments (right graph). Mean cilia length for DMSO (1.41 ± 0.04 μm), forskolin (2.39 ± 0.078 μm), taxol (1.11 ± 0.043 μm), and taxol + forskolin (1.54 ± 0.083 μm). Values as mean ± SEM. Error bars are 95% confidence intervals (see supplemental materials for P values; Table 3). Percentage of cells with cilia in different treatment conditions (left graph, Supplemental materials for P values; Table 4). Histogram of cilia length distribution in different drug conditions (below). (C) Western blot analysis of soluble and polymerized tubulin fractions extracted from IMCD cells after DMSO, taxol only, forskolin only, and taxol + forskolin treatments. Relative amount of tubulin present in soluble and polymerized fractions in each treatment is represented by percent band intensity.

Analysis of ciliogenesis in *IFT88*^{orpk} hypomorphic mutant cells also indicates a role for the cytoskeleton network in cilia elongation

Previously, we demonstrated that partial loss of IFT88 function in *IFT88*^{orpk} hypomorphic mutant mice results in stunted cilia formation (Yoder *et al.*, 2002) and the development of phenotypes associated with ciliopathies, including cystic kidney disease (Lehman *et al.*, 2008). We further evaluated whether actin disruption could rescue the stunted cilia phenotype in these hypomorphic IFT88 mutant cells as previously demonstrated (Kim *et al.*, 2010). In agreement with these previous data, CD-mediated actin disruption was able to restore cilia to normal length in mutant cells (Supplemental Figure S4). We extended these findings by analyzing whether activation of adenylyl cyclase by 0.05 mM forskolin or subtle depolymerization of microtubules with 100 nM nocodazole altered the length of cilia in *IFT88*^{orpk} cells. Intriguingly, as seen with CD, both nocodazole and forskolin increased cilia length (Supplemental Figure S6). Together our findings indicate that ciliogenesis and cilia length can be influenced through the actin cytoskeleton and a pathway involving PKA, both of which are associated with elevated levels of soluble tubulin.

DISCUSSION

Defective assembly or function of primary cilia causes multiple diseases and developmental disorders (Sharma *et al.*, 2008). This recent association between cilia and human disease has increased research and clinical interest into the mechanisms by which cilia are assembled and maintained and how defects in cilia function may influence cellular physiology. Although the length of primary cilia can vary between different tissues or even between cell types within a tissue, it appears that length is under regulatory control as cilia are relatively consistent in size within a specific cell type. This is also observed in the flagella of *Chlamydomonas*, in which multiple genes involved in length control have now been indentified (Wemmer and Marshall, 2007). Whether similar mechanisms exist in mammalian cells is not currently known; however, it seems likely as cells that extended multiple primary cilia in this study were found to have similar length under the different treatment regiments. In addition, it is not known whether signaling activities of the cilium alter its length and morphology as seen in *Caenorhabditis elegans* (Blacque *et al.*, 2004; Mukhopadhyay *et al.*, 2008) or whether increased cilia length can influence a cilium's ability to propagate a signal. It should be noted that multiple cystic kidney disease models involving cilia proteins have been reported and among these are models with either excessively long or short cilia (Taulman *et al.*, 2001; Mokrzan *et al.*, 2007; Tammachote *et al.*, 2009), supporting the idea that abnormal cilia length does have physiological consequences. Furthermore, cilia length in the kidney is markedly increased by acute injury, raising the possibility that cilia are important in regulating or sensing cellular responses to external stresses (Verghese *et al.*, 2008).

The data in this report indicate that there is an important link between the cytoskeleton and regulation of cilia length. Similar to the results reported by Kim *et al.* (2010) when the actin network is destabilized with CD, there was marked increase in cilia length. Here we extend this observation and show that actin stabilization also results in cilia elongation and that there is a concomitant increase in the level of soluble tubulin under these conditions. Importantly, taxol inhibited the effect of actin depolymerization and stabilization, and cilia were also elongated when cells were treated with subtle amounts of nocodazole. These data demonstrate a connection between the levels of soluble tubulin in a cell and the length of its cilium. However, it must be noted that treatment with potent factors, such as nocodazole, taxol, or CD, have wide spanning consequences that may not be directly related to the level of soluble tubulin. For example, changes in cytoskeleton have major effects on membrane and vesicular transport, cell division, cell spreading and migration, cell stress, and responses to mechanical stimuli. Thus at this point it cannot be unequivocally stated that there is a direct connection between the cilia length as observed in our analysis and the levels of soluble tubulin; however, the data do show a strong correlation between these events.

Data shown here, as well as those reported by Kim *et al.* (2010), indicate that actin disruption results in the elongation of cilia. Intriguingly, Kim *et al.* used smoothened-GFP (Smo-GFP) to show that this was associated with the formation of a vesicular structure around

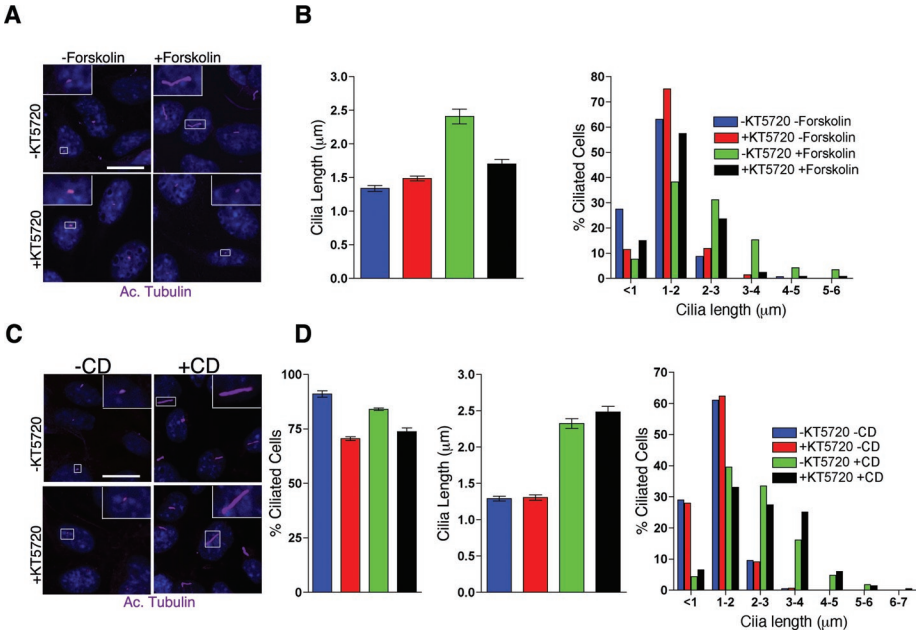

FIGURE 5: Inhibition of PKA suppresses forskolin-induced cilia elongation but not actin depolymerization-induced cilia elongation. (A) PKA inhibitor KT5720 (0.01 mM) blocks forskolin-mediated increase in cilia length. Confocal images are shown of IMCD cells treated with KT5720/forskolin. KT5720 was added 15 min prior to forskolin and then incubated for an additional 3 hours. Cilia were labeled with antibody against acetylated-α-tubulin (Cy5; purple). Scale bar 14 μm and nuclei stained blue with Hoechst. (B) Mean cilia length observed in each treatment paradigm (left graph, from A). Mean cilia length for –KT5720/–forskolin (1.34 ± 0.044 μm), +KT5720/–forskolin (1.484 ± 0.036 μm), –KT5720/+forskolin (2.41 ± 0.11 μm), and +KT5720/+forskolin (1.704 ± 0.066 μm). Error bars are 95% confidence interval (see supplemental materials for P values; Table 5). Cilia length distribution in each treatment paradigm (right graph, from A). (C) KT5720 does not inhibit CD-induced cilia elongation. KT5720 was added 15 min prior to CD treatment and cells were stained with anti-acetylated α-tubulin (purple). Representative confocal images of IMCD cells are shown. Scale bar 14 μm and nuclei stained blue with Hoechst. (D) Mean cilia after each treatment paradigm (from C). Mean cilia length for –KT5720/–CD (1.29 ± 0.033 μm), +KT5720/–CD (1.306 ± 0.037 μm), –KT5720/+CD (2.32 ± 0.066 μm), and +KT5720/+CD (2.48 ± 0.077 μm). Values as mean ± SEM. Error bars are 95% confidence intervals (see supplemental materials for P values; Table 6). Percent of cells with cilia after each treatment paradigm (see supplemental materials for P values; Table 7). Graph showing the distribution of cilia length from each treatment (from C).

the PCC. The PCC is thought to be a site of vesicle docking and a temporary reservoir for ciliary membrane and associated proteins. They conclude in their study that the effect of actin destabilization on cilia length was a result of increased membrane transport into the cilium resulting from the destabilization of the PCC. Although we did not assess the PCC, our data suggest that these effects are also mediated through the microtubule cytoskeleton and increased levels of soluble tubulin, keeping in mind the caveats of the pharmacological approach mentioned above. Further support for a soluble tubulin model in cilia length control comes from recent *Chlamydomonas* studies in which the activity of CrKinesin-13, a cytosolic microtubule-depolymerizing kinesin (mammalian homologue; MCAK), was tightly coordinated with flagella regeneration and establishment of normal flagella length (Piao *et al.*, 2009). Importantly, cells lacking kinesin-13 exhibit a much slower rate of flagella regeneration that is thought to be caused by stabilized cell body microtubules.

Unexpectedly, we found here that both actin stabilization and destabilization caused similar effects with regard to the length of the cilium. In nonmammalian cells in which actin localizes to cilia, disruption of actin results in cilia or flagella shortening (Boisvieux-Ulrich *et al.*, 1990; Dentler and Adams, 1992). Interestingly, CD can induce complete depolymerization of flagellar MTs in *Chlamydomonas* (Dentler and Adams, 1992). Given the actin localization to flagella, it is possible that MT depolymerization might be mediated through actin disruption and thus flagellar shortening in *Chlamydomonas*.

Several studies have identified molecular candidates for mediating structural interactions between actin filament and microtubules in mammalian cells (Rodriguez *et al.*, 2003). For instance, p150 subunit of microtubules motor dynein/dynactin complex colocalizes to F-actin cortical spots and sites of cell–cell contact (Busson *et al.*, 1998) and is involved in centrosome reorientation during cell migration (Levy and Holzbaur, 2008). BBS4, one of the Bardet-Biedl syndrome proteins, localizes to the centrosome/basal body of primary cilia and acts as an adaptor of p150 dynactin to recruit PCM1 (pericentriolar material protein 1) to the centriolar satellites (Kim *et al.*, 2004). Kim *et al.* also showed that silencing of *BBS4* induces mislocalization of PCM1 and disorganized microtubules within the cell body. It should be noted that, later, another study showed that *BBS4* null mice possess longer primary cilia in kidneys and in isolated renal tubules (Mokrzan *et al.*, 2007). These various observations suggest a connection between actin–microtubule structural interactions within the cell body and regulation of primary cilia length. Although we do not yet understand the absolute cellular connection between the actin network and tubulin dynamics, the effect on cilia length correlated directly with soluble tubulin levels and was impaired by treatment with taxol.

In addition to actin depolymerization, several studies have indicated that forskolin can increase cilia length (Low *et al.*, 1998; Besschetnova *et al.*, 2010). This occurred through adenylyl cyclase producing cAMP that in turn activates PKA. The effects of cAMP/PKA on cilia length in Besschetnova *et al.* (2010) were attributed to an increase in the rate of anterograde IFT. Data from our study, as well as from Prasain *et al.* (2009), indicated that cAMP also causes changes in the state of MT polymerization with a concomitant increase in the level of soluble tubulin. Thus it was interesting that cilia elongation in response to forskolin in our analysis was attenuated by taxol, which would prevent the increase in soluble tubulin. The fact that taxol did not completely inhibit cAMP-induced effects supports the idea that cAMP may have multiple influences on cilia length control. As shown by Besschetnova *et al.* (2010), this would include increasing anterograde IFT rates and, as shown here, increased levels of soluble tubulin, the basic building blocks of the cilia axoneme. Taxol would be able to inhibit the liberation of free tubulin induced by cAMP but not the increase in IFT, thus leading to the intermediate cilia length observed.

In contrast to what was observed with forskolin/cAMP, the increase in cilia length caused by actin disruption was not blocked by inhibition of PKA activity. These findings suggest either that PKA functions upstream of actin depolymerization or that there are

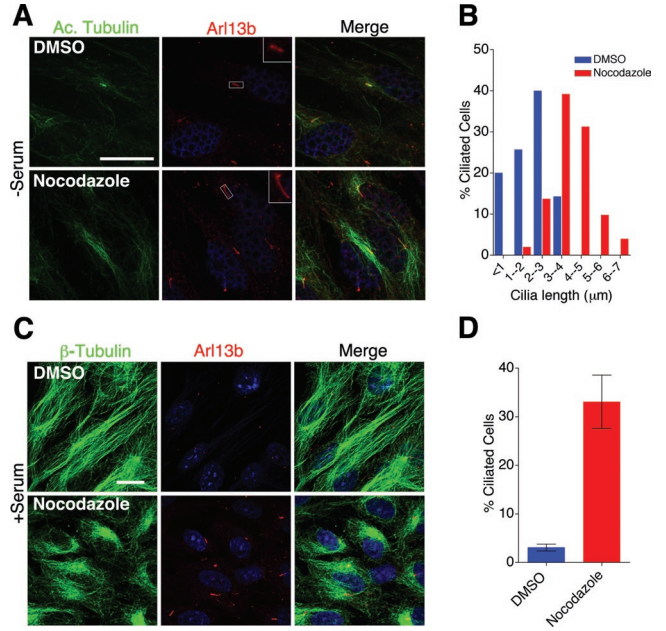

FIGURE 6: Nocodazole-mediated microtubule depolymerization affects cilia length. (A) Forty-eight-hour serum-starved htRPE cells were treated with 100 nM nocodazole for 2 h and stained with antibodies to anti-acetylated α-tubulin (green) and anti-Arl13b (red). Scale bar 15 μm and nuclei stained blue with Hoechst.
(B) Quantification of cilia length distribution in nocodazole-treated cells (from A). Mean cilia length for 100 nM nocodazole (3.9 ± 0.14) and DMSO (1.9 ± 0.15). Values as mean ± SEM. (C) htRPE cells in high-serum growth media were treated with 100 nM nocodazole for 2 h. Cells were stained with anti–β-tubulin (green) and anti-Arl13b (red) antibody to visualize microtubules and cilia. Scale bar 15 μm and nuclei stained blue with Hoechst. (D) Quantification of percentage of ciliated cells (from C). $P < 0.001$.

independent pathways, both of which influence levels of soluble tubulin. The possibility of functioning upstream seems unlikely based on the data indicating that taxol can completely inhibit the cilia length increase caused by actin depolymerization, whereas it does not completely inhibit the cAMP-mediated increase in cilia length. These data again support the possibility that cAMP/PKA has multiple roles in regulation of cilia length.

In our studies, we used taxol to inhibit formation of soluble tubulin. However, Reed *et al.* (2006) have demonstrated that taxol, in addition to stabilizing MTs, also results in enrichment of MT post-translational modifications (Hammond *et al.*, 2010). This was found to alter kinesin-1 trafficking in the cell. Thus we investigated the possibility that the effects of taxol on cilia length in our assays may involve increased PTMs that could subsequently alter the activity of motor proteins, such as the IFT kinesin. This was accomplished by globally increasing tubulin acetylation using inhibitor of HDAC6. Despite a massive increase in the levels of MT acetylation, cilia assembly and length were unaffected. Furthermore, data have shown that over expression of α-tubulin acetyltransferase, mec-17 in *Tetrahymena thermophila* does not affect cilia assembly (Akella *et al.*, 2010). Thus we do not believe that our findings are related to PTMs; however, further studies are needed to evaluate whether other PTMs of tubulin, such as detyrosination, glycylation, or glutamylation, have the ability to alter cilia assembly or length.

Findings reported recently by Besschetnova *et al.* (2010), as well as by us here, indicate that forskolin increases cilia length; however, another study has determined that cilia length can be increased by treatment with lithium chloride (LiCl), but not by forskolin (Ou *et al.*, 2009). Although LiCl is a potent inhibitor of GSK3β, which is known to affect tubulin dynamics (Hong *et al.*, 1997), the proposed mechanism for LiCl by Ou *et al.* (2009) was through inhibition of adenylate cyclase III (AC3). The cause of this discrepancy is not known and may be related to the different cells used in the analyses. Ou *et al.* (2009) analyzed LiCl in fibroblast-like synoviocytes, NIH3T3 cells, astrocytes, and PC12 cells, whereas both our analyses and those by Besschetnova *et al.* (2010) used renal or retinal-pigmented epithelia. In support of this possibility, another recent study has demonstrated that LiCl treatment can cause cilia elongation in some regions of the brain but not others, thus indicating that some cilia respond differently to LiCl than others (Miyoshi *et al.*, 2009).

Here we also show that the stunted cilia observed on cells with reduced IFT ($IFT88^{orpk}$ renal cells) can be rescued by forskolin. $IFT88^{orpk}$ is a hypomorphic allele where anterograde IFT is impaired; thus, based on data from Besschetnova *et al.* (2010) it might be expected that, by increasing the rate of anterograde IFT by cAMP, it would increase cilia length. As shown previously by Kim *et al.* (2010), we also found that CD (as well as nocodazole) increased cilia length in the $IFT88^{orpk}$ mutant cells. In these cases, it is possible that the increase in soluble tubulin precursors resulting from these treatments makes them more readily available for IFT mediated transport into the cilium under the impaired anterograde IFT conditions in the $IFT88^{orpk}$ cells.

In summary, our data show that cilia length can be markedly increased using multiple pharmacological approaches to increase cAMP or to disrupt the actin and microtubule networks. In all of these cases, the increase in cilia length was directly correlated with the levels of soluble tubulin. On the basis of these findings, we propose that one aspect of cilia length control involves regulation of soluble tubulin levels. Further studies will be needed to dissect the mechanisms and signals that the cell uses to balance polymerization/depolymerization state of microtubules and how this influences the length and signaling or sensory capabilities of the cilium.

MATERIALS AND METHODS

Cell culture

Conditional cilia mutant cells lines $CAGGCre^{ER}$; $Kif3a^{fl/fl}$ were generated by microdissection of cortical collecting duct segments from $CAGGCre^{ER}$; $Kif3a^{fl/fl}$; SV40 ImmortoMouse as described (Yoder *et al.*, 2002). Cells were maintained as WT (nontamoxifen-treated) for the present studies. Briefly, the renal collecting tubules were generated by dilute collagenase treatment (0.1 g dl^{-1} collagenase II, 5 mM glycine, 50 U ml^{-1} DNase, in minimal essential medium). Multiple independent clonal cell lines were propagated from selected tubules on collagen-treated culture dishes. Marker analyses indicated that the cells were derived from the collecting duct (data not shown). WT $CAGGCre^{ER}$; $Kif3a^{fl/fl}$ cells were cultured in undifferentiated conditions in collecting tubule medium (CT medium) at 33°C with 5% CO_2 in the presence of interferon-gamma (IFN-γ). CT medium contained the following components: phenol red free DMEM, 5% fetal bovine serum (FBS), 10 ml/l of insulin/selenium/transferrin (ITS at 0.5 mg/ml) solution, 10 μl/l triiodothyronine (T3 at 13 mg/ml), 100 μl/l IFN-γ (IFN-γ at 200 U/ml), and 10 ml/l penicillin–streptomycin (10,000 U/ml penicillin and 10,000 mg/ml streptomycin) antibiotic. IMCD and htRPE cells were maintained in DMEM/F-12 supplemented with 10% FBS. MEFs were isolated and maintained in MEF media (DMEM with 10% FBS, penicillin/streptomycin, primocin, and β-mercaptoethanol). To induce ciliogenesis in htRPE cells and in MEFs, cells were serum starved for 24–48 h. $IFT88^{orpk}$ hypomorphic mutant (94D pCDNA cells) and $IFT88^{rescue}$ cells (94D-Tg737Bap-2)

were derived from the collecting duct, maintained in CT medium, and characterized previously (Yoder *et al.*, 2002).

Antibodies and reagents

For immunofluorescence and immunoblotting, the following antibodies were used: anti-acetylated α-tubulin (Sigma, St. Louis, MO; mouse monoclonal; clone 611B1; 1:1000), anti–α-tubulin (Abcam, Boston, MA; rabbit polyclonal; 1:1000), anti–β-tubulin (Sigma; mouse monoclonal; Clone Tub2.1; 1:1000), anti-Arl13b (a gift from Tamara Caspary, Emory University; rabbit polyclonal; 1:1500), anti-IFT88 (rabbit polyclonal; 1:1000), anti-actin (Sigma; rabbit polyclonal; 1:1000), GT335 antibody (mouse monoclonal; 1:1000, a gift from Carsten Janke, Institut Curie, France). FITC or rhodamine-conjugated goat anti–mouse or goat anti–rabbit secondary antibodies were obtained from Jackson ImmunoResearch (West Grove, PA). Horseradish peroxidase–conjugated goat antibodies to mouse, and rabbit immunoglobulin (Ig)G were obtained from Jackson ImmunoResearch. Forskolin, nocodazole, taxol, CD, and Latrunculin B were purchased from Sigma-Aldrich. Rhodamine–phalloidin (dissolved in methanol; 1:1000) and Jasplakinolide were purchased from Molecular Probes, Invitrogen (Eugene, OR). KT5720 was purchased from Calbiochem (San Diego, CA. Tubacin and niltubacin were generous gifts from Stuart Schreiber (Harvard University).

Cell culture and immunofluorescence

For immunofluorescence, cells were cultured on gelatin-coated coverslips and fixed using a protocol for preservation of cytoskeletal structures (Bell and Safiejko-Mroczka, 1995). Briefly, cells were incubated for 10 min each in Hank's balanced salt solution (HBSS) and MTSB (microtubule stabilizing buffer) containing dithiobis[succinimidylpropionate] (DSP) and then permeabilized and fixed in 0.5% Triton and 4% paraformaldehyde. Cells were incubated with primary antibodies (diluted in 3% bovine serum albumin containing 0.1% normal goat serum) overnight at 4°C followed by 1 h with appropriate secondary antibody at room temperature. Nuclei were visualized by Hoechst staining. Coverslips were mounted with MOWIOL (Fluka Analytical, Milwaukee, WI) or Immunomount (Thermo Fisher, Logan, UT). For β-tubulin staining, cells were fixed and permeabilized in −20°C methanol for 10 min, rehydrated in phosphate-buffered saline (PBS), and processed for immunofluorescence. All images were captured on Perkin Elmer (Waltham, MA) confocal spinning disk microscope, and images were processed and analyzed using Volocity software.

Protein extraction and Western blot

Standard established methods were used for Western blotting (Yoder *et al.*, 2002). Cells were lysed in RIPA buffer, and total protein concentrations were determined by the Bradford assay. Proteins were separated by SDS–PAGE under reducing conditions and transferred onto a nitrocellulose membrane. Membranes were blocked in 5% dry milk and probed with specific primary antibodies and horseradish peroxidase-conjugated secondary antibodies. The proteins recognized by the antibody were visualized by chemiluminescence (Pierce [Rockford, IL] ECL substrate).

To fractionate soluble and polymerized tubulin, soluble tubulin extraction buffer A (137 mM NaCl, 20 mM Tris-HCl, 1% Triton X-100, and 10% glycerol) was added to cells at 4°C for 3 min, plates were gently swirled two to three times, and buffer was removed and saved as soluble fraction. Immediately after, polymerized tubulin extraction buffer B (A + 1% SDS) was added for 1 min, cells were scraped, and the polymerized fraction was sonicated briefly and incubated on ice for 30 min. Soluble and polymerized fractions were quantified by Bradford assay, loaded on a gel, and transferred to nitrocellulose membranes to probe with specific antisera as indicated. Cells treated with nocodazole or taxol alone served as control for efficient extraction of soluble and polymerized tubulin. ImageJ was used to quantify the intensity of α-tubulin and loading protein bands from each blot. Further, the ratio of α -tubulin/loading control was calculated for each soluble (e.g., S_{DMSO}) and polymerized (e.g., P_{DMSO}) lane. The percent band intensity for a particular fraction from each treatment was calculated relative to total tubulin as follows: soluble fraction from DMSO; $[(S_{DMSO})/(S_{DMSO}+ P_{DMSO})] \times 100$ or polymerized fraction from DMSO; $[(P_{DMSO})/(S_{DMSO}+ P_{DMSO})] \times 100$.

Proliferation analysis

For CD and taxol drug treatments, we first established conditions in which the majority of the cell population was in interphase and possessed a consistent length cilium. To ensure significant inhibition of active cell divisions, WT Kif3a$^{fl/fl}$ (nontamoxifen induced, CAGG-Cre^{ER}; Kif3a$^{fl/fl}$) or WT IMCD cells were cultured on coverslips and grown to 80–90% confluency. Cells were washed in PBS and serum starved (0.5% serum) for 72 h. Control cells were left in normal growth media. BrdU labeling reagent was added to serum starved and nonstarved cells. Proliferation index was calculated for starved and nonstarved cells at 2- and 6-h time points. At least 25 cells were counted from 10 randomly captured confocal images in both conditions. A very low proliferation rate was observed in serum-starved cells compared with nonstarved cells, indicating an efficient block in mitosis. These cell culture conditions were applied to later drug treatment experiments to circumvent any effects that mitosis may have on ciliogenesis and cilia length.

Drug treatment experiments

To analyze the effect of actin depolymerization on cilia length, nontamoxifen-induced CAGG-Cre^{ER}; Kif3a$^{fl/fl}$; SV40 cells and WT IMCD cells were treated with 1 μm CD. In subsequent experiments, 1 μm taxol was added for 2 h prior to addition of CD followed by incubation for 3 additional hours. Similarly, IMCD cells were treated with Jaspl to analyze the effect of actin stabilization on cilia length. Also, 1 μm taxol was added for 2 h prior to addition of Jaspl followed by incubation for 3 additional hours. Forskolin, an activator of adenylyl cyclase, was added to cells at 0.05 mM concentration for 3 h to analyze the effects of cAMP and PKA on cilia length. Again, 1 μM taxol was added for 2 h prior to addition of forskolin followed by 3 h of additional incubation. For PKA inhibitor experiments, KT5720 was used at 0.01 mM concentration 15 min prior to the addition of CD or forskolin. Cells were washed in PBS and fixed for immunofluorescence. To assess the effect of microtubule depolymerization upon cilia length, htRPE cells and WT Kif3a$^{fl/fl}$ were treated with 10 nM, 100 nM, and 1 μM nocodazole at 37°C for 2 h.

Rescue of the *IFT88^{orpk}* hypomorphic mutant collecting duct cell cilia

The effect of actin depolymerization on the stunted cilia in hypomorphic, IFT88^{orpk} cells (94D pCDNA cells) (Yoder *et al.*, 2002) was determined by treating cells with 1 μm CD or 0.5 μm Latrunculin B for 3 h. Similarly, IFT88^{orpk} cells were treated with 0.05 mM forskolin or 100 nM nocodazole for 2 h at 37°C.

Quantification and distribution of cilia length measurements

Cells were processed for immunofluorescence microscopy by costaining coverslips with anti-Arl13b and anti-acetylated α-tubulin antibodies. Only cilia double positive for Arl13b and acetylated α-tubulin signal were used for cilia length quantification. At least

25 confocal images were randomly captured from each experiment. Rare incidences of multiciliated cells were evident in CD treatment, and they were excluded from the analysis.

Cilia lengths were measured using confocal stacks and the Volocity Quantification skeletal length measurement. Once cilia lengths were acquired, the data were log transformed to reduce skew and produce a more symmetrical distribution prior to statistical analysis, in order to improve the accuracy of the subsequent statistical tests. P values were obtained using Student's *t* test with unequal variances. To maintain a type I error rate of 0.05 across the multiple comparisons performed, the cut-off for statistical significance was reduced from 0.05 to a rate determined by a sequential Bonferroni correction.

The number of ciliated cells and total number of cells were counted in a given field to determine the percentage of ciliated cells in each treatment. To determine whether these values differed significantly between conditions, P values were obtained using the χ^2 goodness of fit test with contingency tables, and the significance of multiple comparisons was determined using a sequential Bonferroni to maintain a 0.05 type I error rate.

ACKNOWLEDGMENTS

We thank Yoder lab members for helpful suggestions during the progression of this work; Jacek Gaertig (UGA), Corey L. Williams, and Jay Pieczynski (UAB) for critical reading of the manuscript; Tamara Caspary (Emory University) for anti-Arl13b antibodies; and Carsten Janke (Institut Curie, France) for GT335 antibodies. We would also like to thank Stuart Schreiber (Harvard Institute) and Initiative for Chemical Genetics–National Cancer Institute for Tubacin and Niltubacin. This work was funded by NIH grants DK065655 and DK075996 (to BKY) and a National Kidney Foundation postdoctoral fellowship (to NS). ZAK was supported by an NIH T32 GM008111 (to BKY). NFB was supported by NRSA 1F32 DK088484-01. We acknowledge assistance from the NIH-supported Hepato/Renal Fibrocystic Diseases Core Center (UAB HRFDCC, P30 DK074038) to Lisa Guay-Woodford.

REFERENCES

Absalon S, Blisnick T, Kohl L, Toutirais G, Dore G, Julkowska D, Tavenet A, Bastin P (2008). Intraflagellar transport and functional analysis of genes required for flagellum formation in trypanosomes. Mol Biol Cell 19, 929–944.

Akella JS, Wloga D, Kim J, Starostina NG, Lyons-Abbott S, Morrissette NS, Dougan ST, Kipreos ET, Gaertig J (2010). MEC-17 is an alpha-tubulin acetyltransferase. Nature 467, 218–222.

Asleson CM, Lefebvre PA (1998). Genetic analysis of flagellar length control in Chlamydomonas reinhardtii: a new long-flagella locus and extragenic suppressor mutations. Genetics 148, 693–702.

Bell PB Jr, Safiejko-Mroczka B (1995). Improved methods for preserving macromolecular structures and visualizing them by fluorescence and scanning electron microscopy. Scanning Microsc 9, 843–857; discussion 858–860.

Bershteyn M, Atwood SX, Woo WM, Li M, Oro AE (2010). MIM and cortactin antagonism regulates ciliogenesis and hedgehog signaling. Dev Cell 19, 270–283.

Besschetnova TY, Kolpakova-Hart E, Guan Y, Zhou J, Olsen BR, Shah JV (2010). Identification of signaling pathways regulating primary cilium length and flow-mediated adaptation. Curr Biol 20, 182–187.

Blacque OE, Li C, Inglis PN, Esmail MA, Ou G, Mah AK, Baillie DL, Scholey JM, Leroux MR (2006). The WD repeat-containing protein IFTA-1 is required for retrograde intraflagellar transport. Mol Biol Cell 17, 5053–5062.

Blacque OE *et al.* (2004). Loss of C. elegans BBS-7 and BBS-8 protein function results in cilia defects and compromised intraflagellar transport. Genes Dev 18, 1630–1642.

Boisvieux-Ulrich E, Laine MC, Sandoz D (1990). Cytochalasin D inhibits basal body migration and ciliary elongation in quail oviduct epithelium. Cell Tissue Res 259, 443–454.

Bubb MR, Senderowicz AM, Sausville EA, Duncan KL, Korn ED (1994). Jasplakinolide, a cytotoxic natural product, induces actin polymerization and competitively inhibits the binding of phalloidin to F-actin. J Biol Chem 269, 14869–14871.

Bubb MR, Spector I, Beyer BB, Fosen KM (2000). Effects of jasplakinolide on the kinetics of actin polymerization: an explanation for certain in vivo observations. J Biol Chem 275, 5163–5170.

Busson S, Dujardin D, Moreau A, Dompierre J, De Mey JR (1998). Dynein and dynactin are localized to astral microtubules and at cortical sites in mitotic epithelial cells. Curr Biol 8, 541–544.

Chailley B, Bork K, Gounon P, Sandoz D (1986). Immunological detection of actin in isolated cilia from quail oviduct. Biol Cell 58, 43–52.

Chaitin MH, Schneider BG, Hall MO, Papermaster DS (1984). Actin in the photoreceptor connecting cilium: immunocytochemical localization to the site of outer segment disk formation. J Cell Biol 99, 239–247.

Chen XZ, Li Q, Wu Y, Liang G, Lara CJ, Cantiello HF (2008). Submembraneous microtubule cytoskeleton: interaction of TRPP2 with the cell cytoskeleton. FEBS J 275, 4675–4683.

Dawe HR, Adams M, Wheway G, Szymanska K, Logan CV, Noegel AA, Gull K, Johnson CA (2009). Nesprin-2 interacts with meckelin and mediates ciliogenesis via remodelling of the actin cytoskeleton. J Cell Sci 122, 2716–2726.

De Brabander MJ, Van de Veire RM, Aerts FE, Borgers M, Janssen PA (1976). The effects of methyl (5-(2-thienylcarbonyl)-1H-benzimidazol-2-yl) carbamate (R 17934; NSC 238159), a new synthetic antitumoral drug interfering with microtubules, on mammalian cells cultured in vitro. Cancer Res 36, 905–916.

Dentler WL, Adams C (1992). Flagellar microtubule dynamics in Chlamydomonas: cytochalasin D induces periods of microtubule shortening and elongation; and colchicine induces disassembly of the distal, but not proximal, half of the flagellum. J Cell Biol 117, 1289–1298.

Engel BD, Ludington WB, Marshall WF (2009). Intraflagellar transport particle size scales inversely with flagellar length: revisiting the balance-point length control model. J Cell Biol 187, 81–89.

Fliegauf M, Benzing T, Omran H (2007). When cilia go bad: cilia defects and ciliopathies. Nat Rev Mol Cell Biol 8, 880–893.

Gaertig J, Wloga D (2008). Ciliary tubulin and its posttranslational modifications. Curr Top Dev Biol 85, 83–113.

Goswami C, Dreger M, Jahnel R, Bogen O, Gillen C, Hucho F (2004). Identification and characterization of a Ca2+ -sensitive interaction of the vanilloid receptor TRPV1 with tubulin. J Neurochem 91, 1092–1103.

Gundersen GG, Kalnoski MH, Bulinski JC (1984). Distinct populations of microtubules: tyrosinated and nontyrosinated alpha tubulin are distributed differently in vivo. Cell 38, 779–789.

Haggarty SJ, Koeller KM, Wong JC, Grozinger CM, Schreiber SL (2003). Domain-selective small-molecule inhibitor of histone deacetylase 6 (HDAC6)-mediated tubulin deacetylation. Proc Natl Acad Sci USA 100, 4389–4394.

Hammond JW, Huang CF, Kaech S, Jacobson C, Banker G, Verhey KJ (2010). Posttranslational modifications of tubulin and the polarized transport of kinesin-1 in neurons. Mol Biol Cell 21, 572–583.

Holzinger A, Meindl U (1997). Jasplakinolide, a novel actin targeting peptide, inhibits cell growth and induces actin filament polymerization in the green alga Micrasterias. Cell Motil Cytoskeleton 38, 365–372.

Hong M, Chen DC, Klein PS, Lee VM (1997). Lithium reduces tau phosphorylation by inhibition of glycogen synthase kinase-3. J Biol Chem 272, 25326–25332.

Hubbert C, Guardiola A, Shao R, Kawaguchi Y, Ito A, Nixon A, Yoshida M, Wang XF, Yao TP (2002). HDAC6 is a microtubule-associated deacetylase. Nature 417, 455–458.

Ikegami K *et al.* (2007). Loss of alpha-tubulin polyglutamylation in ROSA22 mice is associated with abnormal targeting of KIF1A and modulated synaptic function. Proc Natl Acad Sci USA 104, 3213–3218.

Iomini C, Babaev-Khaimov V, Sassaroli M, Piperno G (2001). Protein particles in Chlamydomonas flagella undergo a transport cycle consisting of four phases. J Cell Biol 153, 13–24.

Johnson KA, Rosenbaum JL (1993). Flagellar regeneration in Chlamydomonas: a model system for studying organelle assembly. Trends Cell Biol 3, 156–161.

Jonassen JA, San Agustin J, Follit JA, Pazour GJ (2008). Deletion of IFT20 in the mouse kidney causes misorientation of the mitotic spindle and cystic kidney disease. J Cell Biol 183, 377–384.

Kim J, Lee JE, Heynen-Genel S, Suyama E, Ono K, Lee K, Ideker T, Aza-Blanc P, Gleeson JG (2010). Functional genomic screen for modulators of ciliogenesis and cilium length. Nature 464, 1048–1051.

Kim JC *et al*. (2004). The Bardet-Biedl protein BBS4 targets cargo to the pericentriolar region and is required for microtubule anchoring and cell cycle progression. Nat Genet 36, 462–470.
Konishi Y, Setou M (2009). Tubulin tyrosination navigates the kinesin-1 motor domain to axons. Nat Neurosci 12, 559–567.
Kozminski KG, Johnson KA, Forscher P, Rosenbaum JL (1993). A motility in the eukaryotic flagellum unrelated to flagellar beating. Proc Natl Acad Sci USA 90, 5519–5523.
Lee E, Shelden EA, Knecht DA (1998). Formation of F-actin aggregates in cells treated with actin stabilizing drugs. Cell Motil Cytoskeleton 39, 122–133.
Lee JC, Field DJ, Lee LL (1980). Effects of nocodazole on structures of calf brain tubulin. Biochemistry 19, 6209–6215.
Lehman JM, Michaud EJ, Schoeb TR, Aydin-Son Y, Miller M, Yoder BK (2008). The Oak Ridge Polycystic Kidney mouse: modeling ciliopathies of mice and men. Dev Dyn 237, 1960–1971.
Levy JR, Holzbaur EL (2008). Dynein drives nuclear rotation during forward progression of motile fibroblasts. J Cell Sci 121, 3187–3195.
Li Q, Montalbetti N, Wu Y, Ramos A, Raychowdhury MK, Chen XZ, Cantiello HF (2006). Polycystin-2 cation channel function is under the control of microtubular structures in primary cilia of renal epithelial cells. J Biol Chem 281, 37566–37575.
Low SH, Roche PA, Anderson HA, van Ijzendoorn SC, Zhang M, Mostov KE, Weimbs T (1998). Targeting of SNAP-23 and SNAP-25 in polarized epithelial cells. J Biol Chem 273, 3422–3430.
Mitchison T, Kirschner M (1984). Dynamic instability of microtubule growth. Nature 312, 237–242.
Miyoshi K, Kasahara K, Miyazaki I, Asanuma M (2009). Lithium treatment elongates primary cilia in the mouse brain and in cultured cells. Biochem Biophys Res Commun 388, 757–762.
Mokrzan EM, Lewis JS, Mykytyn K (2007). Differences in renal tubule primary cilia length in a mouse model of Bardet-Biedl syndrome. Nephron Exp Nephrol 106, e88–96.
Montalbetti N, Li Q, Timpanaro GA, Gonzalez-Perrett S, Dai XQ, Chen XZ, Cantiello HF (2005). Cytoskeletal regulation of calcium-permeable cation channels in the human syncytiotrophoblast: role of gelsolin. J Physiol 566, 309–325.
Montalbetti N, Li Q, Wu Y, Chen XZ, Cantiello HF (2007). Polycystin-2 cation channel function in the human syncytiotrophoblast is regulated by microtubular structures. J Physiol 579, 717–728.
Mukhopadhyay S, Lu Y, Shaham S, Sengupta P (2008). Sensory signaling-dependent remodeling of olfactory cilia architecture in Celegans. Dev Cell 14, 762–774.
Murcia NS, Richards WG, Yoder BK, Mucenski ML, Dunlap JR, Woychik RP (2000). The Oak Ridge Polycystic Kidney (orpk) disease gene is required for left-right axis determination. Development 127, 2347–2355.
Muto E, Edamatsu M, Hirono M, Kamiya R (1994). Immunological detection of actin in the 14S ciliary dynein of Tetrahymena. FEBS Lett 343, 173–177.
Ou Y, Ruan Y, Cheng M, Moser JJ, Rattner JB, Van Der Hoorn FA (2009). Adenylate cyclase regulates elongation of mammalian primary cilia. Exp Cell Res 315, 2802–2817.
Pazour GJ, Wilkerson CG, Witman GB (1998). A dynein light chain is essential for the retrograde particle movement of intraflagellar transport (IFT). J Cell Biol 141, 979–992.
Piao T, Luo M, Wang L, Guo Y, Li D, Li P, Snell WJ, Pan J (2009). A microtubule depolymerizing kinesin functions during both flagellar disassembly and flagellar assembly in Chlamydomonas. Proc Natl Acad Sci USA 106, 4713–4718.
Prasain N, Alexeyev M, Balczon R, Stevens T (2009). Soluble adenylyl cyclase-dependent microtubule disassembly reveals a novel mechanism of endothelial cell retraction. Am J Physiol Lung Cell Mol Physiol 297, L73–83.
Pugacheva EN, Jablonski SA, Hartman TR, Henske EP, Golemis EA (2007). HEF1-dependent Aurora A activation induces disassembly of the primary cilium. Cell 129, 1351–1363.
Quarmby LM, Parker JD (2005). Cilia and the cell cycle? J Cell Biol 169, 707–710.
Reed NA, Cai D, Blasius TL, Jih GT, Meyhofer E, Gaertig J, Verhey KJ (2006). Microtubule acetylation promotes kinesin-1 binding and transport. Curr Biol 16, 2166–2172.
Rodriguez OC, Schaefer AW, Mandato CA, Forscher P, Bement WM, Waterman-Storer CM (2003). Conserved microtubule-actin interactions in cell movement and morphogenesis. Nat Cell Biol 5, 599–609.
Rundle DR, Gorbsky G, Tsiokas L (2004). PKD2 interacts and colocalizes with mDia1 to mitotic spindles of dividing cells: role of mDia1 IN PKD2 localization to mitotic spindles. J Biol Chem 279, 29728–29739.
Saunders C, Limbird LE (1997). Disruption of microtubules reveals two independent apical targeting mechanisms for G-protein-coupled receptors in polarized renal epithelial cells. J Biol Chem 272, 19035–19045.
Scholey JM (2003). Intraflagellar transport. Annu Rev Cell Dev Biol 19, 423–443.
Sharma N, Berbari NF, Yoder BK (2008). Ciliary dysfunction in developmental abnormalities and diseases. Curr Top Dev Biol 85, 371–427.
Sharma N, Bryant J, Wloga D, Donaldson R, Davis RC, Jerka-Dziadosz M, Gaertig J (2007). Katanin regulates dynamics of microtubules and biogenesis of motile cilia. J Cell Biol 178, 1065–1079.
Silflow CD, Rosenbaum JL (1981). Multiple alpha- and beta-tubulin genes in Chlamydomonas and regulation of tubulin mRNA levels after deflagellation. Cell 24, 81–88.
Smith LA, Bukanov NO, Husson H, Russo RJ, Barry TC, Taylor AL, Beier DR, Ibraghimov-Beskrovnaya O (2006). Development of polycystic kidney disease in juvenile cystic kidney mice: insights into pathogenesis, ciliary abnormalities, and common features with human disease. J Am Soc Nephrol 17, 2821–2831.
Sohara E, Luo Y, Zhang J, Manning DK, Beier DR, Zhou J (2008). Nek8 regulates the expression and localization of polycystin-1 and polycystin-2. J Am Soc Nephrol 19, 469–476.
Szymanski D (2002). Tubulin folding cofactors: half a dozen for a dimer. Curr Biol 12, R767–769.
Tammachote R *et al*. (2009). Ciliary and centrosomal defects associated with mutation and depletion of the Meckel syndrome genes MKS1 and MKS3. Hum Mol Genet 18, 3311–3323.
Taulman PD, Haycraft CJ, Balkovetz DF, Yoder BK (2001). Polaris, a protein involved in left-right axis patterning, localizes to basal bodies and cilia. Mol Biol Cell 12, 589–599.
Torres VE, Wang X, Qian Q, Somlo S, Harris PC, Gattone VH, 2nd (2004). Effective treatment of an orthologous model of autosomal dominant polycystic kidney disease. Nat Med 10, 363–364.
Tucker RW, Scher CD, Stiles CD (1979). Centriole deciliation associated with the early response of 3T3 cells to growth factors but not to SV40. Cell 18, 1065–1072.
Tuxhorn J, Daise T, Dentler WL (1998). Regulation of flagellar length in Chlamydomonas. Cell Motil Cytoskeleton 40, 133–146.
Vasquez RJ, Howell B, Yvon AM, Wadsworth P, Cassimeris L (1997). Nanomolar concentrations of nocodazole alter microtubule dynamic instability in vivo and in vitro. Mol Biol Cell 8, 973–985.
Verghese E, Weidenfeld R, Bertram JF, Ricardo SD, Deane JA (2008). Renal cilia display length alterations following tubular injury and are present early in epithelial repair. Nephrol Dial Transplant 23, 834–841.
Watanabe Y, Hayashi M, Yagi T, Kamiya R (2004). Turnover of actin in Chlamydomonas flagella detected by fluorescence recovery after photobleaching (FRAP). Cell Struct Funct 29, 67–72.
Webster DR, Gundersen GG, Bulinski JC, Borisy GG (1987). Assembly and turnover of detyrosinated tubulin in vivo. J Cell Biol 105, 265–276.
Weeks DP, Collis PS (1976). Induction of microtubule protein synthesis in Chlamydomonas reinhardi during flagellar regeneration. Cell 9, 15–27.
Wemmer KA, Marshall WF (2007). Flagellar length control in chlamydomonas–paradigm for organelle size regulation. Int Rev Cytol 260, 175–212.
Wilson NF, Lefebvre PA (2004). Regulation of flagellar assembly by glycogen synthase kinase 3 in Chlamydomonas reinhardtii. Eukaryot Cell 3, 1307–1319.
Yamaguchi T, Nagao S, Kasahara M, Takahashi H, Grantham JJ (1997). Renal accumulation and excretion of cyclic adenosine monophosphate in a murine model of slowly progressive polycystic kidney disease. Am J Kidney Dis 30, 703–709.
Yoder BK, Tousson A, Millican L, Wu JH, Bugg CE Jr, Schafer JA, Balkovetz DF (2002). Polaris, a protein disrupted in orpk mutant mice, is required for assembly of renal cilium. Am J Physiol Renal Physiol 282, F541–F552.